Int. J. Solids Structures, 1973, Vol. 9, pp. 1283 to 1300. Pergamon Press. Printed in Great Britain

STRENGTH OF ECCENTRICALLY LOADED WALLS

W. F. CHEN†

Department of Civil Engineering, Fritz Engineering Laboratory,
Lehigh University, Bethlehem, Pennsylvania 18015, U.S.A.

and

T. ATSUTA‡

Ocean Engineering Department, Kobe Shipbuilding Division, Kawasaki Heavy Industries Ltd., Japan

Abstract—The strength of an eccentrically compressed wall is investigated by treating the wall as a beam–column. The solution adopted is the column-curvature-curve method and the strength is subject to the criteria of stability and strain limits. The material is assumed to be elastic–perfectly plastic. The yield stress levels in tension and compression may be different. Strain limits for cracking and crushing are considered. Thus, the analysis is applicable to materials such as steel, unreinforced concrete, brick and masonry. In selected cases, comparison is made with available and analytical results reported elsewhere and good agreement is observed.

1. INTRODUCTION

WALLS ARE generally treated as compression members in building design. The compressive forces may be applied eccentrically on the walls. Further, bending moments are often induced by rotation of the floor girders. The strength of a wall must hence be investigated using beam-column analysis.

In a recent paper [4] solutions are derived for the computation of elastic deflections and elastic stability of compression members made of materials which exhibit a linear elastic relation between stress and strain in compression and no tensile strength. In Ref. [4], the load is assumed to be applied only at an eccentricity equal to or greater than the kern-eccentricity and smaller than half of the thickness of the member. Herein, a more general solution to this problem will be attempted. In this paper, the material is assumed to be elastic–perfectly plastic and the yield stress levels in tension and compression may be different. In addition, the limited ductility or the strain limits of the material are considered for cracking and crushing. Thus, the analysis is applicable to solid prismatic walls made of masonry, brick or unreinforced concrete as well as metals, since these materials have properties similar to those assumed in this paper. Further, the point of load application may be inside as well as outside the kern-eccentricity region. The Column-Curvature-Curve method (CCC method) developed recently by Chen and Atsuta [2] is used herein to perform the beam–column analysis.

The basic idea of CCC method is the same as that of Column-Deflection-Curve method (CDC method) in which the deflected axis of any column with different end moments can be represented by a portion of the CDC's, but the application of the CCC method is much

† Associate Professor.
‡ Engineer.

simpler. The CCC method was developed in Ref. [2] using analytical curvature solutions due to Chen and Santathadaporn [1], as the consequence, the equivalent column concept is clear and becomes a powerful means to solve moment gradient problems.

For the case of metals, only three cases of equivalent columns cover all possible elastic–plastic beam–columns [2]. Determination of the equivalent column length is the major problem there, for which an iterative procedure is applied. Once the equivalent column length has been known, the curvature distribution is uniquely given in an analytical expression, thus calculation of slope or deflection is straightforward by numerical methods. Herein, the CCC method is extended to consider the materials described in this paper.

2. MATERIAL PROPERTIES

The material considered in this paper is elastic–perfectly plastic as shown in Fig. 1.

E = modulus of elasticity

σ_{ty} = tensile yield stress (positive)

σ_{cy} = compressive yield stress (negative)

ε_{to} = cracking strain (positive)

ε_{co} = crushing strain (negative)

$$\varepsilon_{ty} = \frac{\sigma_{ty}}{E} \qquad \varepsilon_{cy} = \frac{\sigma_{cy}}{E}. \tag{1}$$

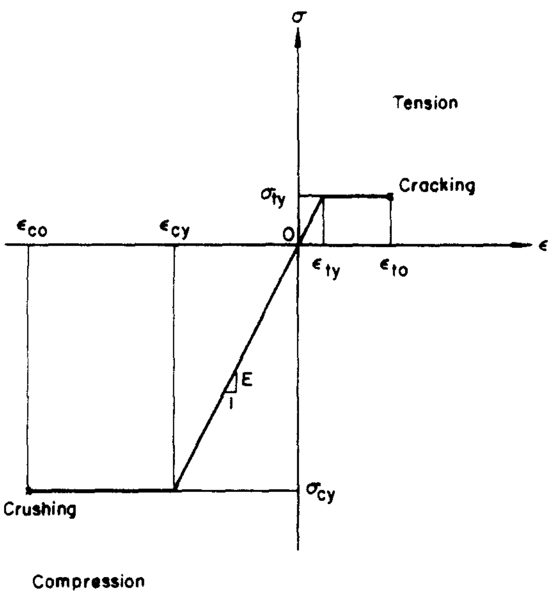

FIG. 1. Idealized stress–strain relationship.

The yield stresses and strain are defined using the ratio μ and the absolute value σ_y of the stress in compression.

$$\sigma_{ty} = \mu\sigma_y \qquad \sigma_{cy} = -\sigma_y \qquad \varepsilon_y = \frac{\sigma_y}{E}. \tag{2}$$

Thus, the analysis is applicable, in general, to materials which have different strengths in tension and in compression.

$$\begin{array}{ll} \text{For idealized steel} & \mu = 1 \\ \text{For idealized masonry} & \mu = 0 \\ \text{For idealized concrete} & 0 < \mu < 1. \end{array} \tag{3}$$

3. MOMENT–CURVATURE–THRUST RELATIONSHIP

The wall has the thickness t and the height h as shown in Fig. 2. The loads are the axial force P on the midthickness and the two end moments M_A and M_B.

The material properties, the geometry and the loads are considered invariant along the width. Hence, a wall with a unit width is considered in this report. Therefore, it is the same as a rectangular beam–column of depth t, width 1·0 and length h.

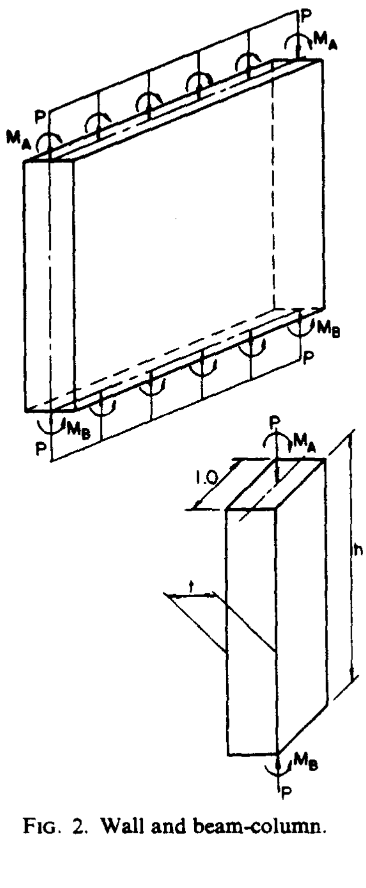

FIG. 2. Wall and beam-column.

It is assumed that plane sections remain plane after deformation. Thus the strain distribution is linear through the wall thickness. In terms of the mean strain ε_m and the curvature Φ (Fig. 3), the strain ε at location y from center line is

$$\varepsilon = \Phi y + \varepsilon_m. \tag{4}$$

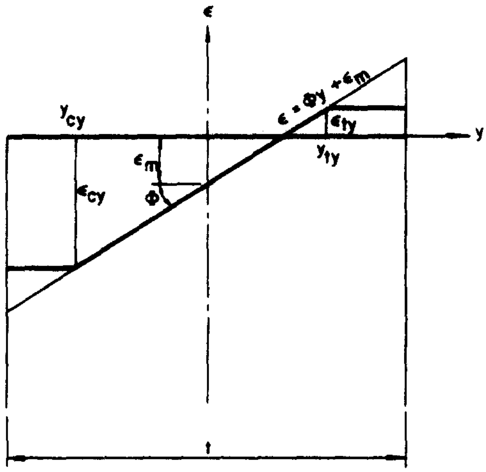

Fig. 3. Linear distribution of strain.

The boundaries of compression yield y_{cy} and tension yield y_{ty} are given by

$$y_{ty} = \frac{1}{\Phi}(\varepsilon_{ty} - \varepsilon_m) \qquad y_{cy} = \frac{1}{\Phi}(\varepsilon_{cy} - \varepsilon_m). \tag{5}$$

Equation (5) has meaning only for

$$-\frac{t}{2} \le y_{ty} \le \frac{t}{2} \qquad -\frac{t}{2} \le y_{cy} \le \frac{t}{2}. \tag{6}$$

The stress is given by

$$\sigma = \begin{cases} \sigma_{cy} & (y \le y_{cy}) \\ E(\Phi y + \varepsilon_m) & (y_{cy} \le y \le y_{ty}) \\ \sigma_{ty} & (y_{ty} \le y). \end{cases} \tag{7}$$

In order to derive simple expressions for axial force P and bending moment M, the following specially defined parentheses are convenient for use.

$$\langle S \rangle = \begin{cases} S & (0 \le S) \\ 0 & (S \le 0). \end{cases} \tag{8}$$

Axial force and bending moment per unit width are

$$P = \int_{-t/2}^{t/2} \sigma \, \mathrm{d}y \qquad M = \int_{-t/2}^{t/2} \sigma y \, \mathrm{d}y. \tag{9}$$

Using equations 7, 8 and 9

$$P = \int_{-t/2}^{t/2} (E\Phi y + E\varepsilon_m)\,\mathrm{d}y - \int_{-t/2}^{t/2} \langle -E\Phi y - E\varepsilon_m + \sigma_{cy} \rangle\,\mathrm{d}y$$

$$- \int_{-t/2}^{t/2} \langle E\Phi y + E\varepsilon_m - \sigma_{ty} \rangle\,\mathrm{d}y \tag{10a}$$

$$M = \int_{-t/2}^{t/2} (E\Phi y + E\varepsilon_m) y\,\mathrm{d}y + \int_{-t/2}^{t/2} \langle -E\Phi y - E\varepsilon_m + \sigma_{cy} \rangle y\,\mathrm{d}y$$

$$- \int_{-t/2}^{t/2} \langle E\Phi y + E\varepsilon_m - \sigma_{ty} \rangle y\,\mathrm{d}y. \tag{10b}$$

These may now be reduced to two simple equations using equations 2, 5 and 8 (Fig. 3),

$$P = E\varepsilon_m t + \frac{E}{2\Phi}\left\langle \frac{\Phi t}{2} - \varepsilon_y - \varepsilon_m \right\rangle^2 - \frac{E}{2\Phi}\left\langle \frac{\Phi t}{2} - \mu\varepsilon_y + \varepsilon_m \right\rangle^2 \tag{11a}$$

$$M = \frac{E\Phi t^3}{12} - \frac{E}{6\Phi^2}\left\langle \frac{\Phi t}{2} - \varepsilon_y - \varepsilon_m \right\rangle^2 (\Phi t + \varepsilon_y + \varepsilon_m)$$

$$- \frac{E}{6\Phi^2}\left\langle \frac{\Phi t}{2} - \mu\varepsilon_y + \varepsilon_m \right\rangle^2 (\Phi t + \mu\varepsilon_y - \varepsilon_m). \tag{11b}$$

The equations are next simplified using nondimensionalized quantities

$$\bar{\sigma} = \frac{\sigma}{\sigma_y} \qquad \bar{\varepsilon} = \frac{\varepsilon}{\varepsilon_y} \tag{12}$$

$$p = -\frac{P}{P_y} \qquad m = \frac{M}{M_y} \qquad \varphi = \frac{\Phi}{\Phi_y} \tag{13}$$

where

$$P_y = \sigma_y t \qquad M_y = \sigma_y \frac{t^2}{6} \qquad \Phi_y = \varepsilon_y \frac{2}{t}. \tag{14}$$

Also, henceforth, a positive value for p indicates compressive force. Thus equation (11) becomes

$$P = -\bar{\varepsilon}_m - \frac{1}{4\varphi}[\langle \varphi - 1 - \bar{\varepsilon}_m \rangle^2 - \langle \varphi - \mu + \bar{\varepsilon}_m \rangle^2] \tag{15a}$$

$$m = \varphi - \frac{1}{4\varphi^2}[\langle \varphi - 1 - \bar{\varepsilon}_m \rangle^2 (2\varphi + 1 + \bar{\varepsilon}_m) + \langle \varphi - \mu + \bar{\varepsilon}_m \rangle^2 (2\varphi + \mu - \bar{\varepsilon}_m)]. \tag{15b}$$

Elimination of $\bar{\varepsilon}_m$ from equations (15a) and (15b) yields a relationship among the bending moment m, the curvature φ and the thrust p in the elastic as well as elastic–plastic regimes.

Since direct elimination is not possible, the m–φ–p equations are derived in four different regimes separately (Fig. 4).

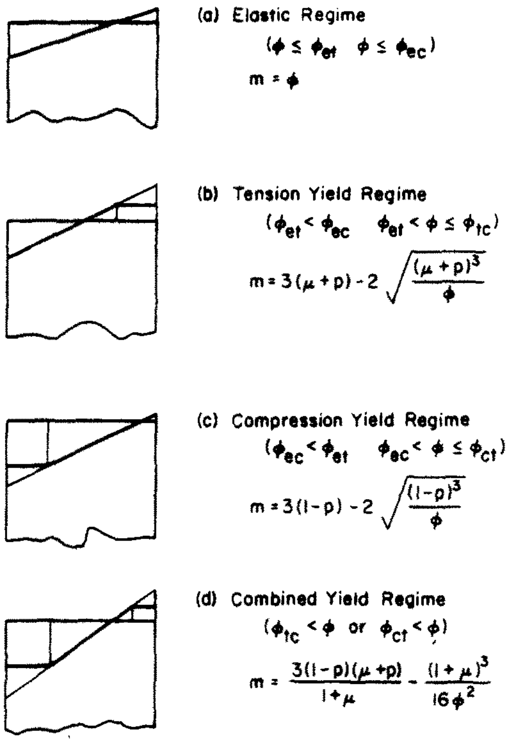

FIG. 4. m–φ–p equations in regimes.

(a) *Elastic regime* ($\varphi \le \varphi_{et}$ and $\varphi \le \varphi_{ec}$)

$$\bar{\varepsilon}_m = -p \tag{16a}$$

$$m = \varphi. \tag{16b}$$

(b) *Tension yield regime* ($\varphi_{et} \le \varphi_{ec}$ and $\varphi_{et} < \varphi \le \varphi_{tc}$)

$$\bar{\varepsilon}_m = \varphi + \mu - 2\sqrt{[\varphi(\mu+p)]} \tag{17a}$$

$$m = 3(\mu+p) - 2\sqrt{\left[\frac{(\mu+p)^3}{\varphi}\right]}. \tag{17b}$$

(c) *Compression yield regime* ($\varphi_{ec} < \varphi_{et}$ and $\varphi_{ec} < \varphi \le \varphi_{ct}$)

$$\bar{\varepsilon}_m = -(1+\varphi) + 2\sqrt{[\varphi(1-p)]} \tag{18a}$$

$$m = 3(1-p) - 2\sqrt{\left[\frac{(1-p)^3}{\varphi}\right]}. \tag{18b}$$

(d) *Combined yield regime* ($\varphi_{tc} < \varphi$ or $\varphi_{ct} < \varphi$)

$$\bar{\varepsilon}_m = \frac{\varphi}{1+\mu}(1-\mu-2p) - \frac{1-\mu}{2} \tag{19a}$$

$$m = 3\frac{(1-p)(\mu+p)}{1+\mu} - \frac{(1+\mu)^3}{16\varphi^2}. \tag{19b}$$

In the present analysis, only positive curvature is taken into account without violating the generality. The boundary curvatures used in equations (16–19) are given by

$$
\begin{aligned}
\varphi_{et} &= \mu + p && \text{(Elastic–tension yield)} \\
\varphi_{ec} &= 1 - p && \text{(Elastic–compression yield)} \\
\varphi_{tc} &= \frac{(1+\mu)^2}{4(\mu+p)} && \text{(Tension–compression yield)} \\
\varphi_{ct} &= \frac{(1+\mu)^2}{4(1-p)} && \text{(Compression–tension yield).}
\end{aligned}
\tag{20}
$$

The order in which the different distributions of stress as shown in Fig. 4(a–d) may occur with increasing φ is of importance in the analysis. If the section is elastic throughout under thrust p alone, its behavior under the bending moment m is initially governed by Fig. 4(a). The addition of the moment m will increase φ and for some value of m, the section will start to yield. Assuming the tension fibers begin to yield first, the behavior is now governed by Fig. 4(b), and the boundary curvature between Fig. 4(a) and Fig. 4(b) is φ_{et}. If the curvature φ can further be increased to φ_{tc}, the compression fibers also begin to yield and for any value of $\varphi > \varphi_{tc}$ the behavior of the section is governed by Fig. 4(d). By similar reasoning, the other sequence of yielding is Fig. 4(a, c) and finally 4(d) and the corresponding boundary curvatures between Fig. 4(a and c) and between Fig. 4(c and d) are φ_{ec} and φ_{ct} respectively.

Comparing the two initial yield curvatures φ_{et} and φ_{ec}, it is known that

$$
\begin{aligned}
&\text{if } p < \frac{1-\mu}{2}, \text{ tension yielding occurs first} \\
&\text{if } p > \frac{1-\mu}{2}, \text{ compression yielding occurs first.}
\end{aligned}
\tag{21}
$$

Using this relationship, equation (20) can be simplified to

$$
\begin{aligned}
\varphi_{et}, \varphi_{ec} &= \frac{1+\mu}{2} - \left|\frac{1-\mu}{2} - p\right| = \varphi_1 \\
\varphi_{tc}, \varphi_{ct} &= \frac{(1+\mu)^2}{4\varphi_1} \qquad\qquad = \varphi_2.
\end{aligned}
\tag{22}
$$

Now there are only three regimes:

(a) *Elastic regime* ($\varphi \leq \varphi_1$)

$$m = a\varphi. \tag{23}$$

(b) *Tension or compression yield regime* ($\varphi_1 < \varphi \leq \varphi_2$)

$$m = b - \frac{c}{\sqrt{\varphi}}. \tag{24}$$

(c) *Combined yield regime* ($\varphi_2 < \varphi$)

$$m = m_{pc} - \frac{f}{\varphi^2} \tag{25}$$

where

$$a = 1 \qquad b = 3\varphi_1 \qquad c = 2\varphi_1^{\frac{3}{2}}$$

$$f = \frac{(1+\mu)^3}{16} \qquad m_{pc} = 3\frac{(1-p)(\mu+p)}{1+\mu}. \tag{26}$$

The m–φ–p relationships derived in Refs [1] and [2] for steel beam-columns and in Refs. [3] and [4] for plain concrete and masonry walls are special cases of equations (23–26) with $\mu = 1{\cdot}0$ and $\mu = 0$ respectively.

4. STRAIN LIMITS

As one of the strength criteria, the wall is assumed to reach its ultimate state when the strain at the extreme fiber reaches the strain limit of the material. The strain limits are

$$\begin{aligned} \varepsilon_{co} &= \text{crushing strain (negative)} \\ \varepsilon_{to} &= \text{cracking strain (positive).} \end{aligned} \tag{27}$$

Since the strain distribution is given by equation (4), these conditions are reached when

$$\begin{aligned} \varepsilon_{co} &= -\frac{\Phi t}{2} + \varepsilon_m \\ \varepsilon_{t0} &= \frac{\Phi t}{2} + \varepsilon_m \end{aligned} \tag{28}$$

or nondimensionally

$$\bar{\varepsilon}_m = \begin{cases} \varphi + \bar{\varepsilon}_{co} \\ -\varphi + \bar{\varepsilon}_{to}. \end{cases} \tag{29}$$

Substituting this $\bar{\varepsilon}_m$ into equations (16–19), the cracking curvature φ_{to} and crushing curvature φ_{co} are obtained as follows:

(a) *Elastic regime* ($\varphi_{to} \leq \varphi_1, \varphi_{co} \leq \varphi_1$)

$$\begin{aligned} \varphi_{to} &= \bar{\varepsilon}_{to} + p \\ \varphi_{co} &= -(\bar{\varepsilon}_{co} + p). \end{aligned} \tag{30}$$

(b) *Tension or compression yield regime* ($\varphi_1 < \varphi_{to} \leq \varphi_2, \varphi_1 < \varphi_{co} \leq \varphi_2$)

$$\begin{aligned} \varphi_{to} &= \frac{\bar{\varepsilon}_{to} + p}{2} + \tfrac{1}{2}\sqrt{[(\bar{\varepsilon}_{to} + p)^2 - (\mu - \bar{\varepsilon}_{to})^2]} \\ \varphi_{co} &= -\frac{(\bar{\varepsilon}_{co} + p)}{2} + \tfrac{1}{2}\sqrt{[(\bar{\varepsilon}_{co} + p)^2 - (1 + \bar{\varepsilon}_{co})^2]}. \end{aligned} \tag{31}$$

(c) *Combined yield regime* ($\varphi_2 < \varphi_{to}, \varphi_2 < \varphi_{co}$)

$$\varphi_{to} = \frac{1}{1-p}\left(\frac{1+\mu}{2}\bar{\varepsilon}_{to} + \frac{1-\mu^2}{4}\right)$$
$$\varphi_{co} = \frac{-1}{\mu+p}\left(\frac{1+\mu}{2}\bar{\varepsilon}_{co} + \frac{1-\mu^2}{4}\right). \tag{32}$$

5. COLUMN-CURVATURE CURVES

For a beam–column AB of length L which is subjected to an axial force P, bending moments M_A and M_B at the ends, there is an equivalent column of length L^* which is subjected only to the axial force

$$P^* = \sqrt{\left[P^2 + \left(\frac{M_A - M_B}{L}\right)^2\right]}. \tag{33}$$

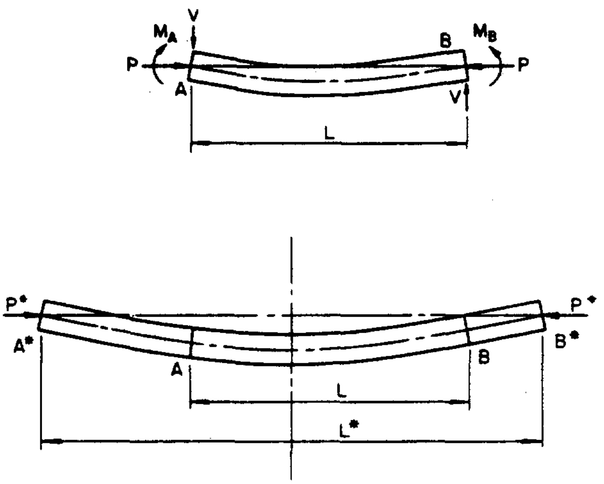

FIG. 5. Beam-column and its equivalent column.

The beam-column AB is a part of its equivalent column A^*B^* as shown in Fig. 5. The proof is presented in Ref. [2].

Since the end curvatures Φ_A and Φ_B are known from end moments M_A and M_B, using the previously obtained moment-curvature–thrust relationship, the curvature distribution along the beam–column AB is determined if the curvature distribution of the equivalent column A^*B^* (the column curvature curves) is known (Fig. 6).

There are five different types of equivalent columns as shown in Fig. 7. The governing equation of a beam–column is

$$\frac{d^2M}{ax^2} + k^2\Phi = 0$$

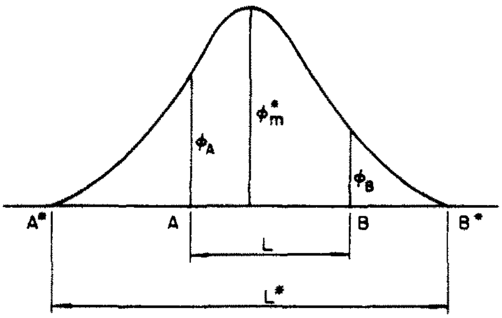

FIG. 6. Curvature of beam-column AB.

in which

$$k = \sqrt{\left(\frac{P^*}{EI}\right)} \tag{35}$$

$$EI = \frac{Et^3}{12} \quad \text{(bending rigidity).} \tag{36}$$

Using the previously derived moment-curvature–thrust relationships, (equations 23–25), equation (34) may be reduced to a set of differential equations in Φ and P only [2].

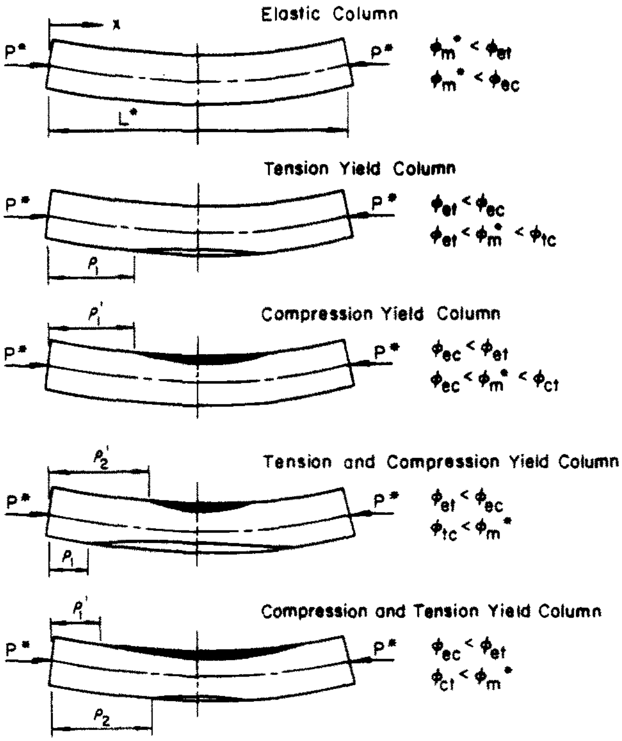

FIG. 7. Five types of equivalent column.

For each type of column shown in Fig. 7, the curvature φ is not solved explicitly. Instead kx is obtained as a function of φ. In the solution, the maximum curvature at the center φ_m^* is included as an integral constant. Details of the solution for each case have been reported elsewhere [2].

If the maximum column curvature φ_m^* is known, the location x_A and x_B corresponding to the end curvatures φ_A and φ_B are obtained exactly from equations (22 to 35) of Ref. [2]. The actual value of φ_m^* must be searched by iteration until the computed length L_{AB} between x_A and x_B becomes close to the length L of the beam-column.

$$L_{AB} \approx L. \tag{37}$$

The length L_{AB} is computed in four different cases as shown in Fig. 8. In each case, the maximum curvature of the beam–column φ_m and its location x_m are given by the following equations.

(a) *Single curvature* ($\varphi_A \varphi_B \geq 0$)
Type 1.

$$\begin{aligned} L_{AB} &= x_B - x_A \\ \varphi_m &= \varphi_A, x_m = 0. \end{aligned} \tag{38}$$

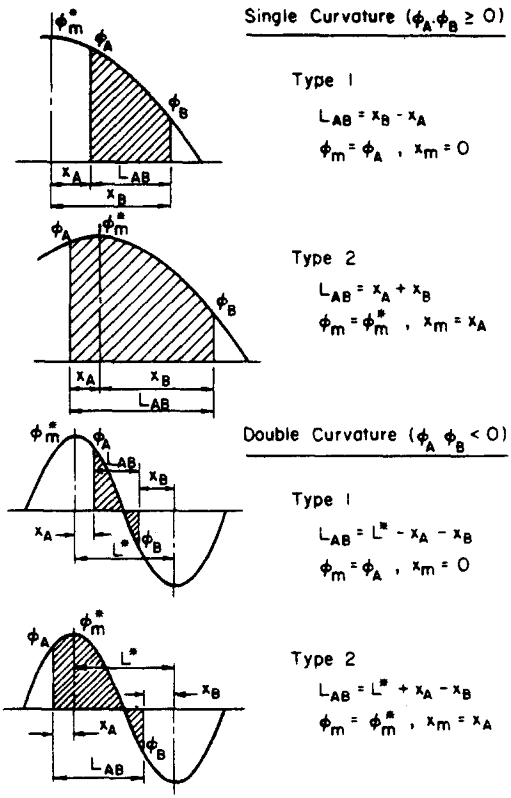

FIG. 8. Computation of column length L_{AB}.

Type 2.

$$L_{AB} = x_B + x_A$$
$$\varphi_m = \varphi_m^*, x_m = x_A. \quad (39)$$

(b) *Double curvature* ($\varphi_A \varphi_B < 0$)

Type 1.

$$L_{AB} = L^* - x_A - x_B$$
$$\varphi_m = \varphi_A, x_m = 0. \quad (40)$$

Type 2.

$$L_{AB} = L^* + x_A - x_B$$
$$\varphi_m = \varphi_m^*, x_m = x_A. \quad (41)$$

In the above derivation, it is assumed (without loss of generality) that

$$|\varphi_B| \leq \varphi_A. \quad (42)$$

6. NUMERICAL EXAMPLES

Results of some numerical calculations are presented in Figs. 9 and 10. The ordinate is the axial force p and the abscissa is the maximum curvature of the wall φ_m. The $p - \varphi_m$ planes are divided by the two dotted lines φ_1 and φ_2 into four regimes: the elastic regime, tension yield regime, compression yield regime and the combined yield regime. The thick

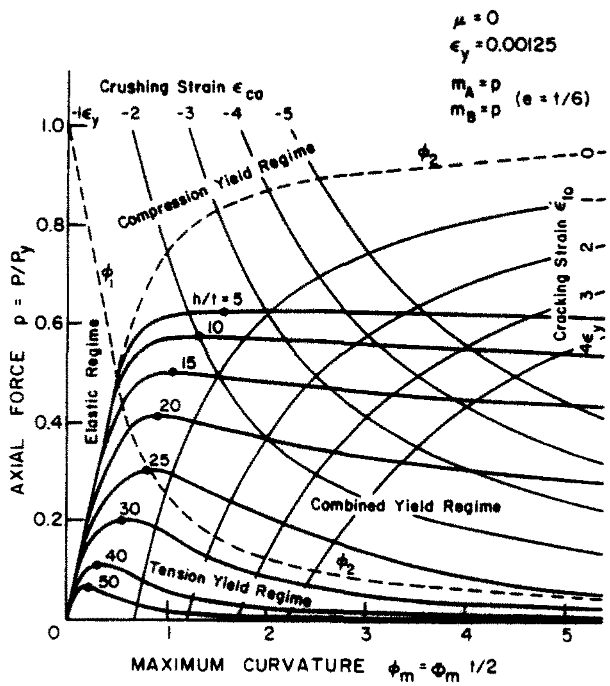

FIG. 9. Load-curvature curves of masonry walls.

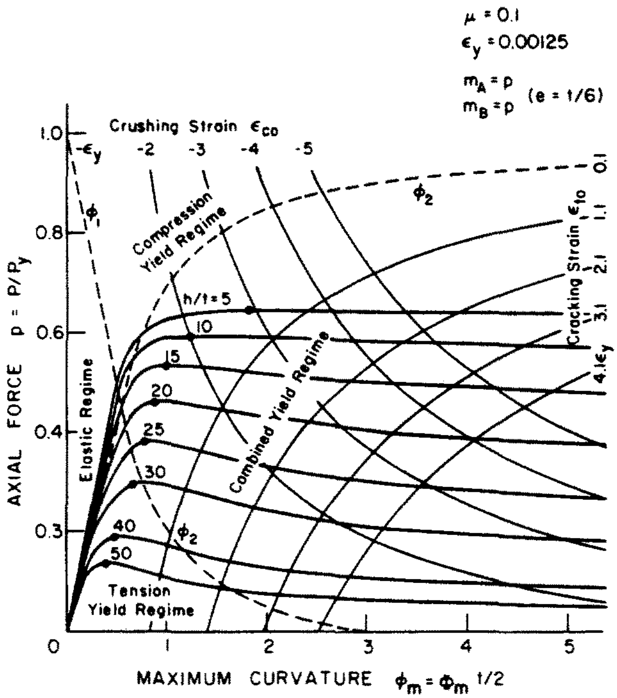

FIG. 10. Load curvature curves of concrete walls.

solid lines represent load curvature curves for various slenderness ratios of h/t. Each curve consists of a loading portion and an unloading portion. The peak points indicate the stability limit of the walls. Strain limits are plotted by thin solid lines.

The stability limits (peak points) occur just after tension yield. Unloading takes place mostly in the combined yield regime except for tall walls with no tensile strength ($\mu = 0$, $h/t > 30$).

Figure 11 shows stability limits of walls with varying tensile strength ($\mu = 0$ to $1{\cdot}0$). It should be noted here that a small amount of tensile strength ($\mu = 0{\cdot}1$) improves the strength of walls considerably. Thus the tensile yield stress should not be neglected in analysis of plain concrete or masonry walls. Tensile yield stress greater than half of compressive yield stress ($\mu > 0{\cdot}5$) has no effect except for very short walls ($h/t < 10$).

Figures 12 and 13 show the ultimate strength of a wall due to strain limits of $\mu = 0$ and $\mu = 0{\cdot}1$ respectively. The thick solid line shows the stability limit. The dotted lines and thin solid lines represent crushing failure and cracking failure, respectively.

Crushing occurs only in shorter walls but cracking occurs in most walls. A small amount of ductility improves the strength of the wall considerably. This effect is noticeable especially during cracking in masonry wall (Fig. 12). Large ductility ($\varepsilon_{to} > 0{\cdot}5\varepsilon_y\, |\varepsilon_{co}| > 2\varepsilon_y$) has little effect on strength of walls.

Figure 14 shows the stability limit of a wall ($\mu = 0$ and $0{\cdot}1$) against different types of loading. The parameter $\mathscr{K}$ is ratio of end moments ($\mathscr{K} = m_B/m_A$). Three loading cases are investigated: symmetric loading ($\mathscr{K} = 1$), one moment loading ($\mathscr{K} = 0$) and anti-symmetric loading ($\mathscr{K} = -1$).

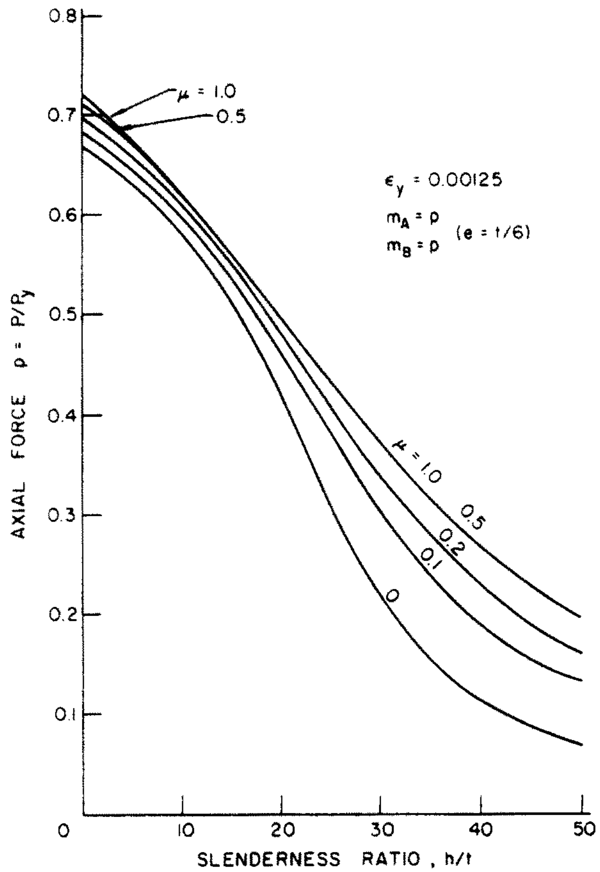

FIG. 11. Strength of wall with various materials.

The strength of the wall under unsymmetric loading ($\mathscr{K} = 0, -1$) is considerably greater than that in the symmetric case. This is because of the difference in the critical length. Also, in these cases, the plastic hinge occurs at an end and the strength becomes constant when the wall is short (Fig. 14).

7. COMPARISON WITH REPORTED RESULTS

In Ref. [4], analytical and experimental ultimal strengths of walls are reported. In the analytical part Yokel [4] assumes that the material has no tensile strength ($\mu = 0$). The compressive crushing strain limit ε_{co} is the same as the initial yield strain ε_{cy} ($\varepsilon_{co} = \varepsilon_{cy} = -\varepsilon_y$) and the tensile strain limit is not defined ($\varepsilon_{to} = \infty$). The loading is symmetric ($\mathscr{K} = 1$) but eccentricity of the axial force is variable ($e = t/6$ and $e = t/3$ are taken in the example). The yield strain is $\varepsilon_y = 0{\cdot}001215$ in pure compression. Strength in flexure is assumed to be 1·6 times the strength in pure compression ($\varepsilon_y = 0{\cdot}001944$). Results of Ref. [4] are plotted by open circles in Fig. 15.

To recompute these analytical results using the approach here, the ultimate strength of the walls is investigated in four cases. In Fig. 15, the solid curves (a) and (b) represent

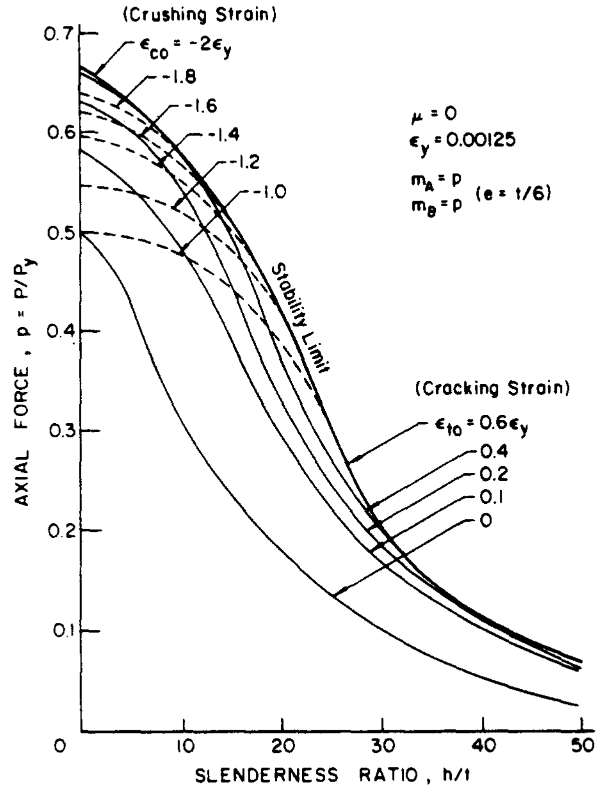

FIG. 12. Ultimate strength due to strain limits.

stability limits of the walls with $\varepsilon_y = 0{\cdot}001215$ and $\varepsilon_y = 0{\cdot}001944$, respectively. Since there are strain limits ($\varepsilon_{co} = \varepsilon_{cy} = -\varepsilon_y$), the strengths are reduced to the dotted lines (a′) and (b′). Applying the factor 1·6 to the p-value of the curve (b′), the crushing strength curve (c) is obtained. The ultimate strength is represented by the stability part of curve (a) and crushing part of curve (c). Figure 15 shows good agreement between the two analytical results in both cases of eccentricity. It should be emphasized, however, that the experimental results reported by Yokel [4] showed a considerable scatter about his analytical curves, especially for the case $e = t/3$.

8. SUMMARY AND CONCLUSIONS

A method to analyze strength of walls of general materials is presented. An elastic–perfectly plastic material is considered. The yield stresses and limited ductility or strains in tension and compression may be different. In the analysis, the column-curvature-curve method is used.

The loadings are axial compression and bending moments at the ends, which may be unsymmetric. Further, the end moments are not necessarily due to eccentricity of the axial force, they may be applied independently.

The small tensile strength and ductility of plain concrete or masonry are found to have a significant effect on the strength of walls and should not be neglected in analysis. For

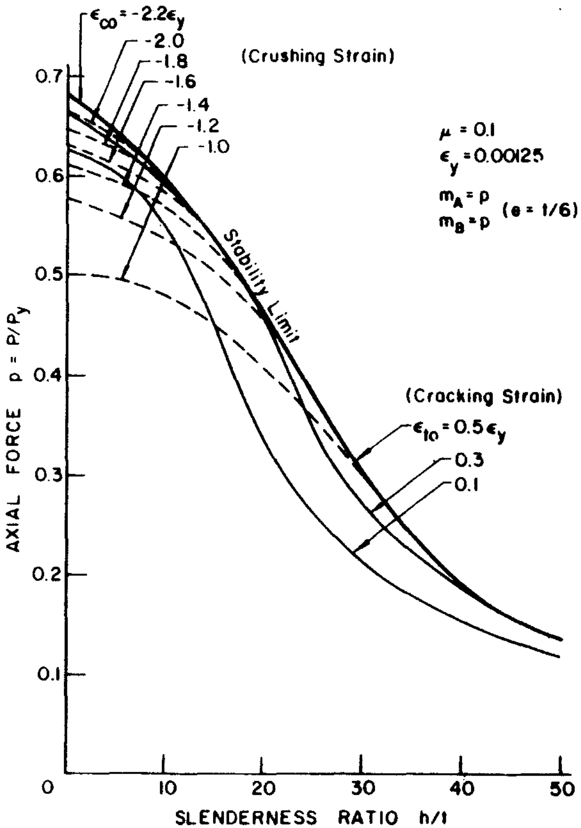

FIG. 13. Ultimate strength due to strain limits.

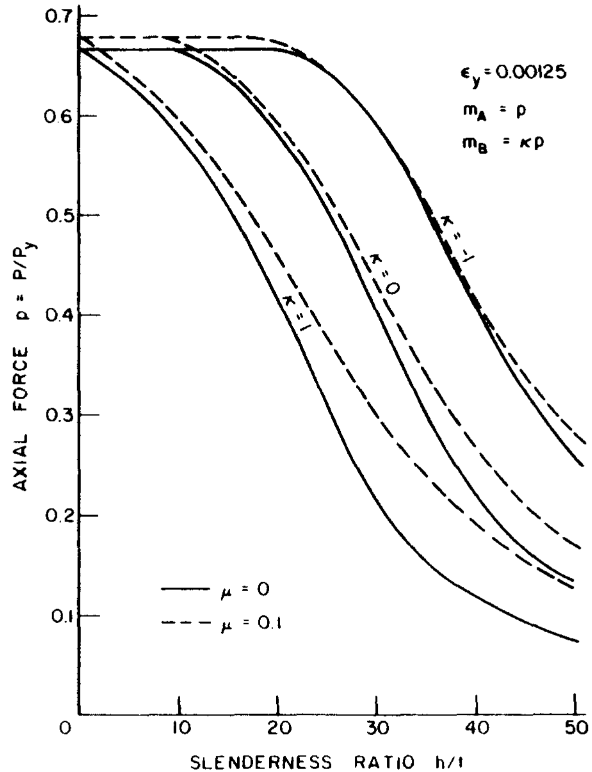

FIG. 14. Strength of wall against various types of loading.

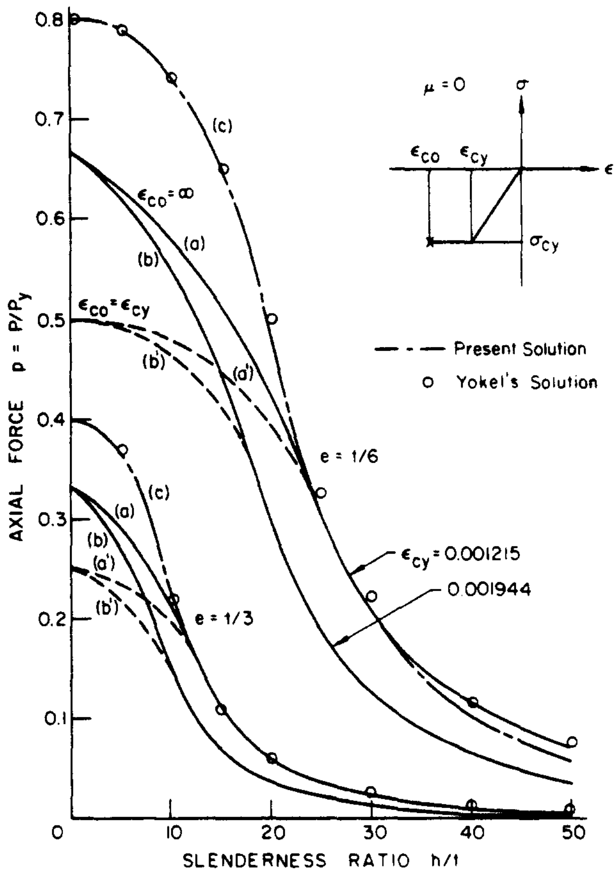

FIG. 15. Comparison with Ref. [4].

unreinforced concrete, brick or masonry walls, compressive ductility greater than twice the initial yield strain ε_y and tensile ductility greater than half the initial yield strain ε_y are desirable features.

A good agreement was observed in some special cases with other reported results.

Acknowledgements—T. Atsuta is grateful to Kawasaki Heavy Industries, Ltd., Japan for providing him with the opportunity to study at Lehigh University. The preparation of this report was sponsored by the National Science Foundation under Grant GK-35886 to Lehigh University. All computations were made at the Computer Center through the Department of Civil Engineering, Lehigh University.

REFERENCES

[1] W. F. Chen and S. Santathadaporn, Curvature and solution of eccentrically loaded columns. *J. Engng Mech. Div. ASCE* **95**, 21 (1969).

[2] W. F. Chen and T. Atsuta, Column curvature curve method for analysis of beam columns. *J. Inst. Struct. Engrs* **50**, 233 (1972).

[3] W. F. CHEN, Discussion of: Stability and load capacity of members with no tensile strength, (F. Y. YOKEL). *J. Struct. Div. ASCE* **98**, 1193 (1972).
[4] F. Y. YOKEL, Stability and load capacity of members with no tensile strength. *J. Struct. Div. ASCE* **97**, 1913 (1971).

(*Received* 4 *January* 1973; *revised* 4 *April* 1973)

Абстаркт—Исследуется сопротивление эксцентрипно сжатой стены, обсуждая эту стену в виде балки-колонны. Принятое решение является методом кривой изгиба колонны и сопротивление подчиняется критериям устойчивости и пределам деформации. Предполагается материал упруго-идеальнопластический. Уровни пластических напряжений для сжатия и растяжения могут быть разные. Рассматриваются пределы деформации для образования трещин и раздавливания. Затем анализ можно использовать к поведению таких материалов, как сталь, неармированный бетон, кирпич или кирпичная кладка. Для избранных случаев, дается сравнение с доступными аналитическми результатами, предложенными где нибудь в другом месте, и наблюдается надлежащее согласие.